A.-C. Wong, H. Ding, and C. T.-C. Nguyen, "Micromechanical mixer+filters," *Technical Digest*, IEEE International Electron Devices Meeting, San Francisco, California, Dec. 6-9, 1998, pp. 471-474.

Micromechanical Mixer+Filters

Ark-Chew Wong, Hao Ding, and Clark T.-C. Nguyen

Center for Integrated Sensors and Circuits
Department of Electrical Engineering and Computer Science
University of Michigan
Ann Arbor, Michigan 48109-2122

ABSTRACT

A device comprised of interlinked micromechanical resonators with capacitive mixer transducers has been demonstrated to perform both low-loss frequency translation (i.e. mixing) and highly selective filtering of applied electrical input signals. In particular, successful down-conversion of radio frequency (RF) signals from 40-200MHz and subsequent filtering at a 27MHz intermediate frequency (IF) with less than 15dB of combined mixing conversion and filter insertion loss is demonstrated using this single, micromechanical device. Mixing conversion gain/loss is shown to depend upon a ratio of local oscillator amplitude and applied bias voltages. A single-sideband (SSB) noise figure of 18dB is achieved.

I. INTRODUCTION

Super-heterodyne communication receivers rely heavily on both highly selective filtering and low-loss, low-noise mixing for frequency channel selection and down-conversion. To maximize performance, these mixing and filtering functions are most often achieved via separate and distinct components that must interface with one another at the board-level. The use of separate components for mixing and IF filtering not only places limits on the degree of size reduction possible in portable communication devices, but can also entail added power consumption if special drivers are required to properly match the output of the mixer to the subsequent filter. Furthermore, impedance mismatches between the mixer output and filter input can contribute additional insertion loss in the receive path.

Recent advances in micromachining technologies that yield high-*Q* micromechanical resonators [1] may now offer a method for combining both of these functions into a single passive, micro-scale device. This paper reports on such a device comprised of interlinked micromechanical resonators with capacitive mixer transducers that down-converts radio frequency (RF) signals from 40-200MHz to a 27MHz intermediate frequency (IF), then performs high-*Q* filtering, all with less than 15dB of combined mixing conversion and filter insertion loss, and with ideally zero dc power consumption. Such a device can potentially replace both the filtering and mixing functions in heterodyning wireless communication transceivers (as shown in Fig. 1), reducing both size (by orders of magnitude) and power dissipation over the off-chip macroscopic counterparts often used in current systems.

II. MIXER+FILTER STRUCTURE AND OPERATION

Figure 2(a) presents a schematic describing the structure and operation of the micromechanical mixer+filter device. As shown, the basic structure of this device mimics that of a μmechanical filter [2], comprised of two clamped-clamped beam μresonators, each with center frequency f_{IF}, coupled at low-velocity locations by a flexural mode beam. As such, the device operates by first converting an electrical input signal to a mechanical force, then processing this signal mechanically via its network of flexural-mode beams, then re-converting the resulting signal to an electrical output signal that can be further processed by subsequent transceiver electronics. This structure, however, differs from previous filters in that the coupling beam is now highly resistive to reducing local oscillator-to-output coupling, and additional electrodes have been provided to allow voltage-controlled frequency tuning and localized annealing [3] for each μresonator. In addition, the gaps between the electrodes and resonators are now only 300Å in order to maximize electromechanical couplings at the input and frequency pulling transducers.

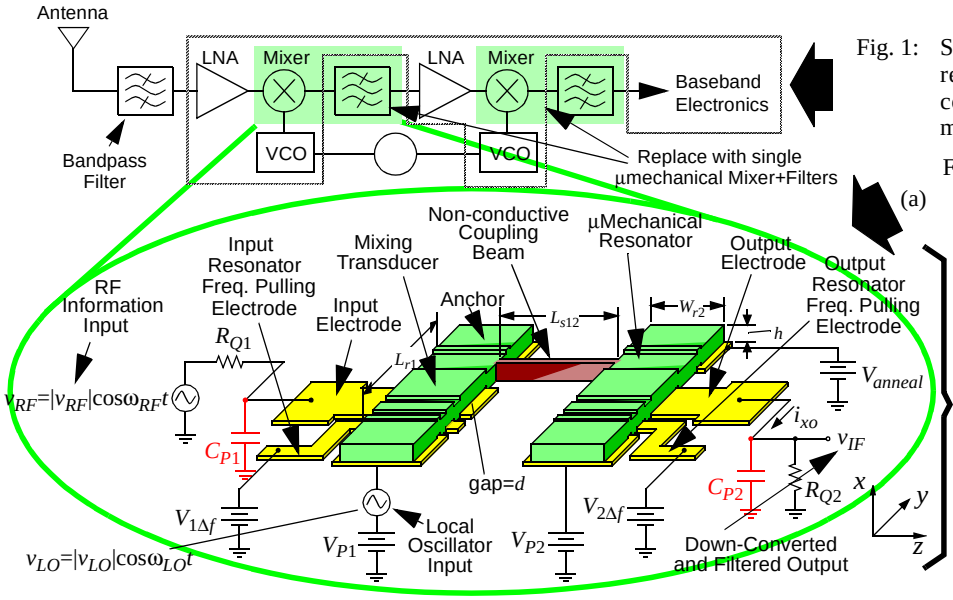

Fig. 1: Simplified block diagram of a wireless receiver, indicating (with shading) the components replaceable by the subject mixer+filter devices.

Fig. 2: (a) Schematic diagram of the described μmechanical mixer+filter, depicting the bias and excitation scheme needed for down-conversion. (b) Equivalent block diagram of the mixer+filter scheme.

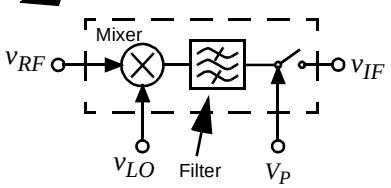

To operate this device as a mixer+filter, very specific input placements are required: a local oscillator input v_{LO} with frequency f_{LO} applied to the input resonator; an information (or RF) input v_{RF} with frequency $f_{RF}=f_{IF}+f_{LO}$ (consistent with actual inputs to communication transceivers) applied to the terminated input electrode; and a dc-bias voltage V_P applied to the input and output resonators in the filter structure. Even though none of the applied signals shown in Figure 2(a) is within the passband of the micromechanical filter, a *force* component *within* the filter passband still arises at the input due to quadratic nonlinearity in the voltage-to-force capacitive input transducer. Specifically, this force F_i is given by: (assuming $V_{P1}=V_{P2}=V_P$, which will be the case henceforth)

$$\begin{aligned} F_i &= \frac{1}{2}(V_P + v_{LO} - v_{RF})^2(\partial C_1/\partial x) \\ &= \ldots - v_{LO}v_{RF}\frac{\partial C_1}{\partial x} + \ldots \\ &= \ldots - \frac{1}{2}|v_{LO}||v_{RF}|\frac{\partial C_1}{\partial x}\cos(\omega_{RF}-\omega_{LO})t + \ldots \end{aligned} \quad (1)$$

where dC_1/dx is the incremental change in electrode-to-resonator capacitance at the input transducer (and is negative in sign), and where the mixed component of interest has been singled out. The frequency of the force falls within the filter passband when $f_{RF}=f_{LO}+f_{IF}$, at which point vibration is induced in the micromechanical filter section, and a subsequent filtered signal is generated by the dc-biased, time varying capacitor at the output transducer. This output signal will have a frequency within the IF passband around f_{IF} and a current magnitude into the output resistor R_{Q2} given by

$$i_{xo} = V_P\frac{\partial C_2}{\partial x}\frac{\partial x}{\partial t} \quad (2)$$

where dC_2/dx is the incremental change in electrode-to-resonator capacitance at the output transducer.

III. MIXER+FILTER DESIGN

The design specification for this device encompasses both mixer and filter requirements, and thus, includes metrics for IF frequency f_{IF}, filter bandwidth B, filter shape factor S, and overall noise figure F. As explained in [2], when the resonators are identical, the center frequency of the filter f_{IF} is equal to the center frequency of each resonator, which with tuning electrodes is now given by the expression

$$f_{IF} = \frac{1}{2\pi}\kappa\sqrt{\frac{k_r}{m_r}} = \frac{1}{2\pi}\kappa\sqrt{\frac{k_{mio}}{m_r}}\left(1 - \langle\frac{k_{ei}}{k_m}\rangle - \langle\frac{k_{eit}}{k_m}\rangle\right)^{1/2}, \quad (3)$$

where k_r and m_r are the effective stiffness and mass, respectively, at the I/O location ($y=L_r/2$) of each μresonator [2], κ is a fitting parameter that accounts for beam topography and finite elasticity in the anchors, k_{mio} is the *mechanical* stiffness of each μresonator at the I/O location, and $\langle k_{ei}/k_m\rangle$ and $\langle k_{eit}/k_m\rangle$ are mechanical-to-electrical stiffness ratios integrated over the I/O and tuning electrode lengths, respectively, of resonator i, and satisfying the relations (assuming $|v_{LO}|>>|v_{RF}|$)

$$\langle\frac{k_{ei}}{k_m}\rangle = \int_{\frac{1}{2}(L_r-W_e)}^{\frac{1}{2}(L_r+W_e)}\frac{(V_P^2 + 0.5|v_{LO}|_i^2)\varepsilon_o W_r}{d^3k_m(y')}dy' \quad (4)$$

$$\langle\frac{k_{eit}}{k_m}\rangle = 2\int_{l_{ta}}^{l_{tb}}\frac{((V_P - V_{i\Delta f})^2 + 0.5|v_{LO}|_i^2)\varepsilon_o W_r}{d^3k_m(y')}dy', \quad (5)$$

where ε_o is the permittivity in vacuum, $k_m(y)$ is the location-dependent *mechanical* stiffness [2], W_e is the width of the I/O electrodes, l_{ta} and l_{tb} are the y-locations of the tuning electrode edges measured from the anchors, other geometric dimensions are given in Figs. 2(a) and 3, $|v_{LO}|_i\approx 0$V for i=2, and where tuning electrodes are assumed to be placed symmetrically around I/O electrodes in (5). The bandwidth B of the filter is given by the expression

$$B = \left(\frac{f_{IF}}{k_{12}}\right)\left(\frac{k_{s12}}{k_r}\right), \quad (6)$$

where k_{s12} is the stiffness of the coupling beam, and k_{12} is a normalized coupling coefficient found in filter cookbooks [5]. To attain a properly flattened passband, termination resistors are required as shown in Fig. 2(a), given by

$$R_{Q1} = R_{Q2} = \frac{\omega_{IF}m_r}{Q\eta_e^2}\left(\frac{Q}{qQ_{fltr}} - 1\right), \quad (7)$$

where η_e is the electromechanical coupling factor of the I/O transducers, Q is the resonator quality factor, $Q_{fltr}=(f_{IF}/B)$, and q is a normalized Q value found in filter cookbooks [5].

Conversion Gain/Loss.

The mixer conversion gain/loss in this device is determined primarily by the relative magnitudes of the dc-bias V_P applied to the resonator and the local oscillator amplitude $|v_{LO}|$. Using (1), assuming R_{Qn} resistors given by (7), and with the recognition that the filter structure presents a large input impedance to both v_{RF} and v_{LO} (since their frequencies are off-resonance), the expression for conversion gain/loss takes the form

$$G_{conv} = \frac{1}{L_{conv}} = \frac{|v_{LO}|}{V_P} \rightarrow 20\log\left[\frac{|v_{LO}|}{V_P}\right] \text{ [dB]}. \quad (8)$$

Note that conversion gain is possible if $|v_{LO}| > V_P$.

Noise Figure.

The SSB noise figure for this device derives from a combination of mixer conversion loss, filter insertion loss, and an additional 3dB that accounts for noise conversion from two bands (RF and image) to one [4], and can be expressed as

$$F = L_{conv}|_{\text{dB}} + L_{fltr}|_{\text{dB}} + 3 \text{ [dB]}, \quad (9)$$

where $L_{fltr}|_{\text{dB}}$ is the filter insertion loss in dB. Possible values might be $L_{conv}|_{\text{dB}}$=0dB (with $|v_{LO}|=V_P$) and $L_{fltr}|_{\text{dB}}$=2dB, leading to F=5dB—very good calculated performance for a combined mixer and filter using passive components.

IV. FABRICATION

Micromechanical mixer+filters were designed using the above procedure, then fabricated using a polysilicon surface-micromachining process that was conventional [1] in all respects, except for an extra implant blocking mask to define high-resistance (~5MΩ) coupling beams and a much thinner sacrificial oxide to define structure-to-substrate gap spacings of only 300Å. Such small gaps significantly impacted the fabrication and performance of the devices as follows:

(1)A substantially longer sacrificial release etch in hydrofluoric acid (HF)—45 min. on average—was required to free

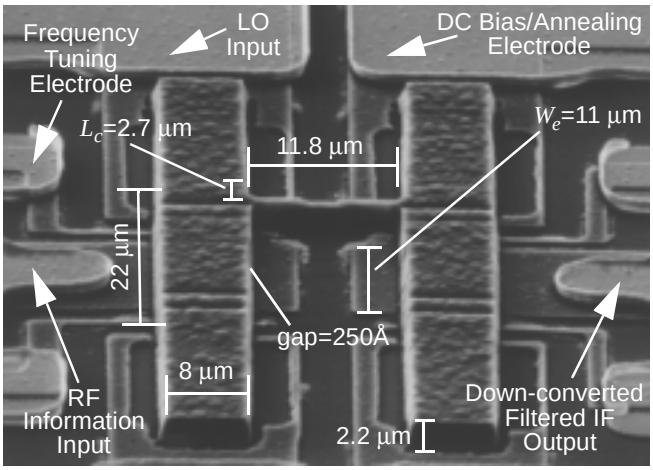

Fig. 3: SEM of the 27MHz μmechanical mixer+filter with important dimensions.

the devices. This resulted in attack of interconnect polysilicon and raised the series resistance of the leads to electrodes. Although Cr/Au metallization helped to reduce interconnect resistance, it could not cover all interconnect areas. As a consequence, interconnect resistances up to 200Ω degraded resonator *Q*'s by up to a factor of ten.

(2) Extensive cleaning procedures, including piranha cleans and supercritical CO_2 cleaning, were required after release to clear out etch by-products from the tiny gaps.

(3) During testing, the *Q* of small-gapped resonators was quite sensitive to contamination by contaminants (e.g., pump oil molecules), more so than previous large- gapped resonators. Contamination in the gap is suspected as a damping mechanism for these small-gapped devices, and strict environmental control is stressed to minimize it.

Figure 3 presents scanning electron micrographs (SEM's) of a 27MHz IF mixer+filter device, indicating key dimensions and features. Device yield was limited mainly by residues remaining in the tiny electrode-to-resonator gaps after the HF release etch. Again, extensive cleaning procedures were required to improve yields.

V. EXPERIMENTAL RESULTS

To minimize parasitic capacitance, mixer+filters, as well as stand-alone resonators and filters, were attached and bonded directly to circuit boards containing the needed electronics shown in Fig. 2(a), then evaluated in a custom-built vacuum chamber under 50μTorr pressure (provided by a turbo-molecular pump). Even at this low pressure, contaminants are still suspected in the system, perhaps due to outgassing from the board and electronics.

An HP 8714C Network Analyzer was used with the above chamber and electronics to obtain frequency spectra for the stand-alone resonators and filters. The measured frequency spectrum for a 49.7MHz μresonator is shown in Fig. 4, showing a directly measured *Q* of 2,000. Due to insufficient environmental control in the test apparatus used, elevated temperatures were required to remove contaminants from the device surfaces and from the electrode-to-resonator gaps, which otherwise severely compromised device *Q*'s. For many of the resonators tested, high *Q* was seen only after the temperature of the resonator was raised via a localized annealing procedure, in which an electric current is pushed through the resonator device to heat it up [3].

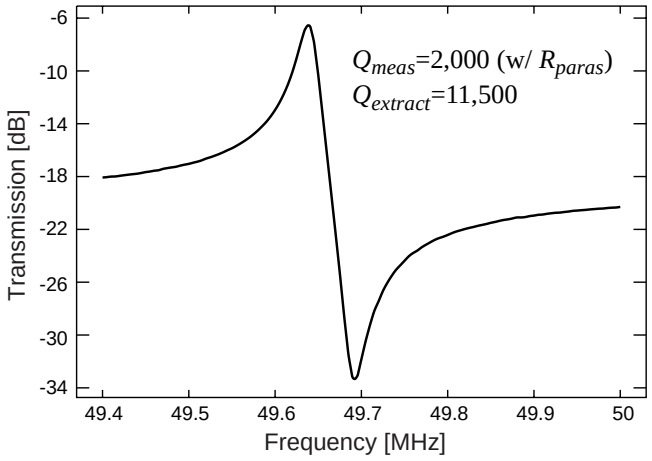

Fig. 4: Frequency spectrum for a 49.7MHz clamped-clamped beam micromechanical resonator measured under 50 μTorr vacuum. $Q_{extract}$ accounts for interconnect R_{paras}.

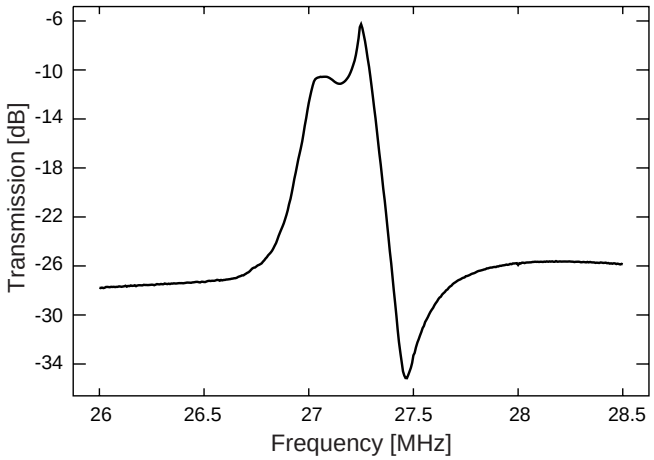

Fig. 5: Frequency characteristic for a 27MHz micromechanical filter measured under 50 μTorr vacuum.

The measured *Q* shown in Fig. 4 is not the intrinsic *Q* of the resonator device by itself. Rather, it represents a *Q* value loaded by series resistance from the polysilicon interconnect. Taking into account series resistance in the interconnect and electronics (~150Ω+250Ω) and using a calculated value for resonator series resistance R_x=84Ω, the theoretical actual value of resonator *Q* is found to be 11,500. Of course, a filter comprised of such resonators does not see this "actual" resonator *Q*; rather, its performance will be degraded by interconnect resistance, as well. Figure 5 presents the measured frequency characteristic for a 27MHz two-resonator filter, showing 6dB of insertion loss for a 0.86% bandwidth (*B*=233kHz), with 20dB of stopband rejection, and a 20dB-down shape factor of 2.65. Although adequate for IF applications, this does not convey the true potential of this technology. In particular, smaller insertion loss should be achievable with more conductive interconnects.

Mixer+filter devices were then tested, again using the custom-built vacuum chamber, but with the set-up shown in Fig. 6. Here, the output of a mixer+filter device is monitored in the IF range (24-29MHz) by a spectrum analyzer in MAX HOLD mode while the device is driven by an RF signal v_{RF} swept from 37-42MHz, with a 13MHz local oscillator voltage v_{LO} applied. The procedure for evaluating mixer+filters was as follows:

(1) Apply an annealing voltage across each resonator to

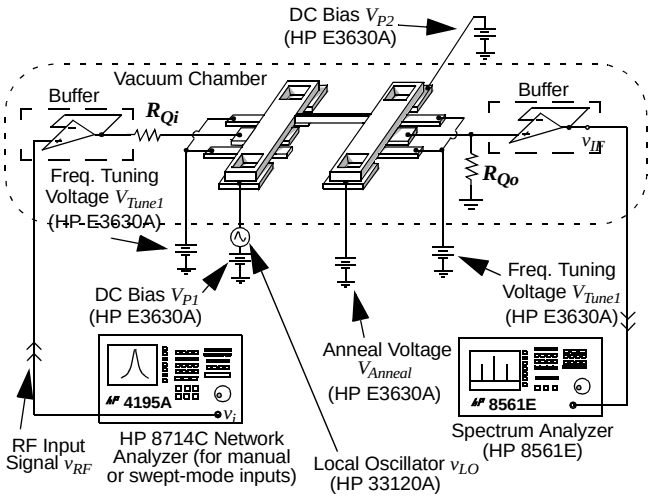

Fig. 6: Experimental set-up for mixer+filter evaluation.

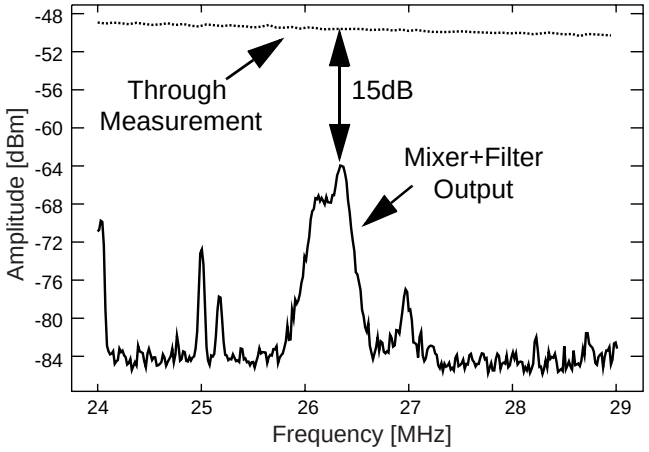

Fig. 7: Spectrum obtained when sweeping the RF input v_{RF} over a 37-42MHz frequency range while detecting and holding outputs (using the MAX HOLD function on an HP 8561E Spectrum Analyzer) over a 24-9MHz range. Note the frequency shift from Fig. 5 due to the addition of the local oscillator signal (c.f., Eqs. (4) and (5)).

remove contaminants, then measure a first spectrum;

(2) adjust tuning voltages to move mode peaks to the desired bandwidth;

(3) adjust the LO amplitude and the dc-bias voltage to flatten out the spectrum, iterating with step (2) if necessary to obtain a properly flattened passband.

The result of this procedure is shown in Fig. 7, which shows the output spectrum of the mixer+filter under RF excitation, as measured by a spectrum analyzer in MAX HOLD mode. The fact that the IF filter spectrum is seen as output under RF excitation clearly indicates down-conversion and filtering. Table I summarizes the excitation signal levels used and performance obtained via this evaluation. A through measurement, in which the mixer+filter device is bypassed by a short-circuit, is also included in Fig. 7. From the difference between this curve and the IF spectrum's peak signal, the total combined mixer conversion and filter insertion loss is 15dB. Considering the 6dB filter insertion loss measured in Fig. 5, the conversion loss is 9dB, which is consistent with the prediction of (8) when using V_P and $|v_{LO}|$ values from Table I. Successful down-conversion was also demonstrated for RF frequencies up to 200MHz, but these showed much more conversion loss than the data presented in Fig. 7, mainly due to the unavailability of a high frequency function generator able to source voltage amplitudes larger than 1V— i.e., $|v_{LO}| << V_P$ in these measurements.

Table I: μMechanical Mixer+Filter Evaluation Data

Parameter	Value	Units
μResonator Mass @ I/O, m_r	3.54×10^{-11}	kg
μResonator Stiffness @ I/O, k_r	10,194	N/m
Coupling Beam Stiffness, k_{s12}	1,206	N/m
Electrode-to-Resonator Overlap	88	μm^2
Electrode-to-Resonator Gap, d	300	Å
Electromechanical Coupling, η_e	1.12×10^{-5}	C/m
IF Center Frequency	27	MHz
IF Filter Bandwidth	233	kHz
20dB-down Shape Factor	2.65	—
Filter Insertion Loss	6	dB
Mixer Conversion Loss	9	dB
LO-to-IF Isolation (f_{LO}=13MHz)	13	dB
LO-to-RF Isolation (f_{LO}=13MHz)	13.5	dB
RF-to-IF Isolation (f_{RF}=42MHz)	16	dB
$\|v_{RF}\|$ (swept from 37-42MHz)	–15	dBm
$\|v_{LO}\|$ (13MHz)	5.5	V
Resonator DC-Bias, V_P	21	V
Termination Resistance, R_{Q1}=R_{Q2}	2,200	Ω

Finally, the LO-to-IF, LO-to-RF, and RF-to-IF isolations were also measured and are summarized in Table I. Due to the lack of a substrate ground plane in this particular process, these data are not representative of the true isolation capabilities of this technology. Devices utilizing more creative shielding strategies are currently under investigation.

VI. CONCLUSIONS

Micromechanical mixer+filter devices have been demonstrated with IF frequencies in the low VHF range and SSB noise figures around 18dB— performance on par with other discrete, passive mixer/filter combinations. Down-conversion and filtering of RF signals from 40-200MHz has been achieved. The need for large voltages, both ac magnitudes and dc bias levels, remains an issue for the mixer+filters of this work, but can be alleviated in future versions if smaller electrode-to-resonator gaps (~200Å) or circuit+μstructure integration (which decreases node capacitance, thus, allowing higher R_{Qn} values) are utilized. The use of such smaller gaps coupled with more conductive interconnect should allow mixer+filter devices with substantially better noise figure than demonstrated here. Finally, the contamination-induced *Q*-degradation seen in this work stresses the need for controlled environments (perhaps provided by a combination of vacuum encapsulation and temperature control) when using micro-scale mechanical devices.

References:

[1] W. C. Tang, *et al*., *Sensors and Actuators*, **BA21-A23**, pp. 328-331, 1990.

[2] F. D. Bannon III, *et al*., *IEDM*'96, pp. 773-776, 1996.

[3] K. Wang, *et al*., *Tranducers'97*, pp. 109-112, 1997.

[4] B. Razavi, *RF Microelectronics*. Prentice Hall PTR, 1998.

[5] A. I. Zverev, *Handbook of Filter Synthesis*. Wiley, 1967.